CHIN.PHYS.LETT. Vol. 25, No. 3 (2008) 870

Synchronized Anti-Phase and In-Phase Oscillations of Intracellular Calcium Ions in Two Coupled Hepatocytes System *

SHEN Chuan-Sheng(申传胜)[1,2], CHEN Han-Shuang(陈含爽)[2], ZHANG Ji-Qian(张季谦)[2]**

[1]*Department of Educational Technology, Anqing Teachers College, Anqing 246011*

[2]*College of Physics and Electronic Information, Anhui Normal University, Wuhu 241000*

(Received 10 November 2007)

We study the dynamic behaviour of two intracellular calcium oscillators that are coupled through gap junctions both to Ca^{2+} and inositol(1,4,5)-trisphosphate (IP_3). It is found that synchronized anti-phase and in-phase oscillations of cytoplasmic calcium coexist in parameters space. Especially, synchronized anti-phase oscillations only occur near the onset of a Hopf bifurcation point when the velocity of IP_3 synthesis is increased. In addition, two kinds of coupling effects, i.e., the diffusions of Ca^{2+} and IP_3 among cells on synchronous behaviour, are considered. We find that small coupling of Ca^{2+} and large coupling of IP_3 facilitate the emergence of synchronized anti-phase oscillations. However, the result is contrary for the synchronized in-phase case. Our findings may provide a qualitative understanding about the mechanism of synchronous behaviour of intercellular calcium signalling.

PACS: 05. 45. Xt, 05. 45. −a, 05. 40. −a

As a second messenger in living cells, calcium ions play a vital role in providing the intracellular signalling. Many important cellular processes and biological function, such as muscle contraction and synaptic transmission, are regulated by Ca^{2+} signals.[1−3] In hepatocytes, oscillatory intercellular Ca^{2+} waves are generated by the coupling of intracellular Ca^{2+} oscillations[4,5] in response to vasopressin,[6,7] and these waves also occur in the blowfly salivary gland;[8] a plausible hypothesis is that these waves are the result of intercellular coupling by means of the diffusion of Ca^{2+} through gap junctions. Yule *et al.*[9] showed that these gap junctions are permeable to inositol (1,4,5)-trisphosphate (IP_3) and Ca^{2+}. Wu *et al.*[10] demonstrated that sufficient and continuous IP_3 level is necessary for the synchronization of IP_3-induced Ca^{2+} oscillations in coupled hepatocytes, and observed a gradual transition from synchronous behaviour to nonsynchronous behaviour. Recently, they observed that there exist an optimal coupling strength and an optimal stimulation level for the synchronization. In addition, Politi *et al.*[11] found that IP_3R plays a positive role and exerts negative feedback of Ca^{2+} on the IP_3 metabolism.

In the last two decades, intracellular calcium dynamics of different theoretical models are proposed.[12−16] The phenomena that the IP_3 concentration can oscillate together with cytoplasmic calcium can also be observed experimentally.[17−19] It is well known that hormone-evoked calcium dynamics in hepatocytes involves the interplay of calcium fluxes from and into the ER and across the plasma membrane, and possibly also other compartments such as mitochondria. We aim to analyse the dynamics of coupled cells, so a relatively simple model proposed by Höfer is applied in this study.[4] The model involves calcium release fluxes from the ER (denoted by $J_{\rm rel}$), calcium reuptake through the sarco/endoplasmic reticulum calcium ATPase ($J_{\rm SERCA}$), the calcium fluxes across the plasma membrane ($J_{\rm in}$ and $J_{\rm out}$), and the gap-junctional flux. In this work, Choosing the coupling strength of Ca^{2+} and IP_3 as control parameters, by calculating numerically, we study the effects of these parameters on synchronous behaviour and discuss the possible biological significance of our findings in living systems.

In view of the fact that, in the model, IP_3 can diffuse through gap junctions, its progression over time needs to be considered in the description of the Ca^{2+} dynamics in each hepatocyte. To this end, we incorporate in the model a general equation describing synthesis of IP_3 by phospholipase C (PLC) and IP_3 metabolism by IP_3 3-kinase and 5-phosphatase.[19] Introducing the coupling effects both of $Ca^{2+}$and IP_3, the time evolutions of Ca^{2+} in the cytoplasm, in the whole cell and the concentration of IP_3 in the two cells (denoted by $x_{1,2}$, $z_{1,2}$, and $P_{1,2}$, respectively) are given by

$$\begin{aligned}\frac{dx_{1,2}}{dt} &= \rho[(J_{\rm in}-J_{\rm out})+\alpha(J_{\rm rel}-J_{\rm SERCA})] \\ &\quad +\gamma_{\rm Ca}(x_{2,1}-x_{1,2}), \\ \frac{dz_{1,2}}{dt} &= \rho(J_{\rm in}-J_{\rm out})+\gamma_{\rm Ca}(x_{2,1}-x_{1,2}),\end{aligned}$$

*Supported by the Educational Commission of Anhui Province of China under Grant No KJ2007A079, the Research Fund for Young Teachers in Colleges of Anhui Province under Grant No 2007jql118, the Research Fund of Anhui Normal University under Grant No 2006xzx09, and the Programme for Innovative Research Team of Anhui Normal University.

**Email: zhangcdc@mail.ahnu.edu.cn

© 2008 Chinese Physical Society and IOP Publishing Ltd

$$\frac{dP_{1,2}}{dt} = V_{\rm PLC} - V_K \frac{P_{1,2}}{K_K + P_{1,2}} \frac{x_{1,2}^2}{K_d + x_{1,2}^2} - V_{\rm PH} \frac{P_{1,2}}{K_{PH} + P_{1,2}} + \gamma_{\rm IP}(P_{2,1} - P_{1,2}). \quad (1)$$

Here a conservation of the total cellular Ca^{2+} implies the constraint $z_{1,2} = x_{1,2} + \beta y_{1,2}$; y denotes the free calcium concentration in the ER. $V_{\rm PLC}$ is the velocity of IP_3 synthesis by PLC, which depends on the level of stimulation; $\gamma_{\rm Ca}$ and $\gamma_{\rm IP}$ are Ca^{2+} and IP_3 junctional coupling strength, respectively. The other abbreviations are defined by

$$\begin{aligned} J_{\rm in} &= v_0 + v_c \frac{P_{1,2}}{K_0 + P_{1,2}}, \quad J_{\rm out} = v_4 \frac{x_{1,2}^2}{K_4^2 + x_{1,2}^2}, \\ J_{\rm SERCA} &= v_3 \frac{x_{1,2}^2}{K_3^2 + x_{1,2}^2}, \\ J_{\rm rel} &= k_r(x_{1,2}, P_{1,2}) \Big(\frac{z_{1,2} - x_{1,2}}{\beta_i} - x_{1,2} \Big) \\ k_r(x_{1,2}, P_{1,2}) &= k_1 [d_2(d_1 + P_{1,2}) P_{1,2} x_{1,2}]^3 \\ &\cdot \{(d_p + P_{1,2})(d_a + x_{1,2}) \\ &\cdot [d_2(d_1 + P_{1,2}) + x_{1,2}(d_3 + P_{1,2})]\}^{-3} + k_2. \end{aligned} \quad (2)$$

The meaning and numerical value of the kinetic parameters are given in Table 1.

Table 1. Parameters remain unchanged in the following section.

P	Value	Meaning
ρ	$0.02\mu M^{-1}$	Ratio of plasma membrane area/ cytosol volume
α	2	Ratio of areas ER/plasma membrane
β	0.1	Ratio of effective volumes ER/cytosol
v_0	$0.2\mu Ms^{-1}$	Constant influx(Ca^{2+})
v_c	$4.0\mu Ms^{-1}$	Maximal rate of calcium entry increases with P
v_3	$9.0\mu Ms^{-1}$	Maximal SERCA pump rate
v_4	$3.6\mu Ms^{-1}$	Maximal PMCA pump rate
V_K	$0.075\mu Ms^{-1}$	Maximal velocity of IP_3 metabolism by 3-kinase
d_a	$0.4\mu M$	Ca^{2+} binding to activating site
d_p	$0.2\mu M$	IP_3 binding
d_1	$0.3\mu M$	Dissociation constant for IP_3
d_2	$0.4\mu M$	Dissociation constant for Ca inhibition
d_3	$0.2\mu M$	Receptor dissociation constant for IP_3
k_1	$40.0s^{-1}$	Rate constant of maximal IP_3 R-mediated release
k_2	$0.02s^{-1}$	Rate constant of a small leak flux
K_0	$4.0\mu M$	IP_3 binding
K_3	$0.12\mu M$	Half-activation constant
K_4	$0.12\mu M$	Half-activation constant
K_K	$1.0\mu M$	Michaelis constant characterizing the 3-kinase
K_d	$0.5\mu M$	Threshold constant for IP_3 3-kinase activation by Ca^{2+}
$K_{\rm PH}$	$10.0\mu M$	Michaelis constant characterizing the 5-phosphatase
$V_{\rm PH}$	$0.075\mu Ms^{-1}$	Maximal velocity of IP_3 metabolism by 5-phosphatase

Equations (1) and (2) are calculated numerically with time steps $dt = 0.01$ s. To obtain each numerical result, we perform 50 runs which have different initial conditions. At each run, the first 10^6 time steps are discarded to achieve steady state and 10^6 time steps are used to investigate the dynamics of the system.

Before beginning the investigation of the coupled system, it will be useful to analyse the bifurcation property of an uncoupled cell. The bifurcation diagram for the cell system and the period of calcium oscillations as functions of $V_{\rm PLC}$ are shown in Fig. 1. One can notice that this diagram shows the steady states and oscillatory solutions as well as their stabilities, with the increment of $V_{\rm PLC}$, the cell system undergoes two Hopf bifurcation points at $V_{\rm PLC} \approx 0.0106\,\mu$M/s (left bifurcation point (LBP)) and $V_{\rm PLC} \approx 0.045\,\mu$M/s (right bifurcation point (RBP)), respectively. For $V_{\rm PLC} < 0.0106\,\mu$M/s there is a single stable steady state; as $V_{\rm PLC}$ is increased, two unstable steady states appear between LBP and RBP (dot-dashed line). Finally, as $V_{\rm PLC}$ further increases, the unstable steady states disappear and a fixed point gains stability in RBP, then it remains stable as $V_{\rm PLC}$ continues upward. The dependence of the period of unstable periodic orbits on $V_{\rm PLC}$ are also shown in Fig. 1.(circle). Thus, from this figure, we may obtain some useful clues for understanding the mechanism of anti-phase or in-phase synchronization, those results are shown in the following section in this paper.

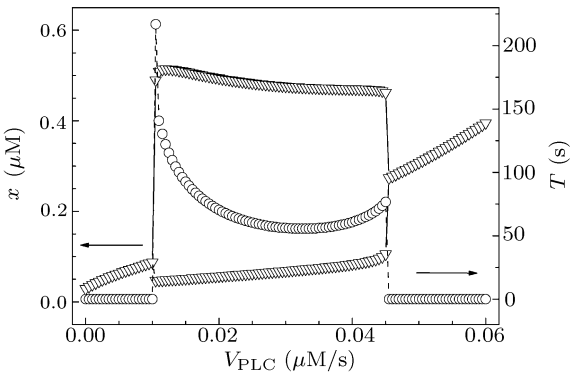


Fig. 1. Bifurcation diagram for an uncoupled cell. The stable (unstable) states are denoted with solid circles (open circles). The dependence of the period of unstable periodic orbits on $V_{\rm PLC}$ (right axis).

To characterize quantitatively synchronous behaviour of the system, a phase is introduced into each cell: $\phi_i(t) = 2\pi \dfrac{t - \tau_k^i}{\tau_{k+1}^i - \tau_k^i} + 2\pi k$, where τ_k^i is the time of the kth spike in ith cell, which is determined by the threshold value of $x_i(t)$ at $x_i(t) = 0.3\,\mu$M. Then, we calculate the quantity $\Delta\phi = \langle |\phi_1(t) - \phi_2(t)| \rangle$, for measuring phase difference between the two cells. Here, the marks $|\cdots|$ and $\langle \cdots \rangle$ denote the absolute value and the averaging over time, respectively. Obviously, the phase difference of the two cells is deemed to be in-phase synchronization if $\Delta\phi = 0$ and anti-phase synchronization while $\Delta\phi = \pi$.

Next, we consider the effects of $V_{\rm PLC}$ and $\gamma_{\rm IP}$ in the absence of gap junction to calcium. The curves of $\Delta\phi$ as a function of $V_{\rm PLC}$ for three different $\gamma_{\rm IP}$ are plotted in Fig. 2. One can notice that, on the one hand, $\Delta\phi$ keeps a constant $\Delta\phi = \pi$ if the value of $V_{\rm PLC}$ is near LBP. However, when $V_{\rm PLC}$ is increased from LBP to a certain value, $\Delta\phi$ suddenly becomes zero (e.g. $V_{\rm PLC} \approx 0.011\,\mu$M/s for $\gamma_{\rm IP} = 0.1$). Specially, if $V_{\rm PLC}$ is further increased, $\Delta\phi$ will always keep $\Delta\phi = 0$. Thus, synchronous anti-phase oscillations can be achieved when the value of $V_{\rm PLC}$ is slightly larger than LBP. This indicates that when $V_{\rm PLC}$ exceeds a critical value, the system may undergo the transition from anti-phase oscillations to in-phase ones. On the other hand, by comparing the results of Figs. 2(a)–2(c), one can observe that the region of anti-phase oscillations is enlarged for a larger $\gamma_{\rm IP}$. In Fig. 3, we plot typical time evolutions of Ca^{2+} and IP_3 in the cytoplasm. It provides us with an intuitive illustration of in-phase and anti-phase synchronization.

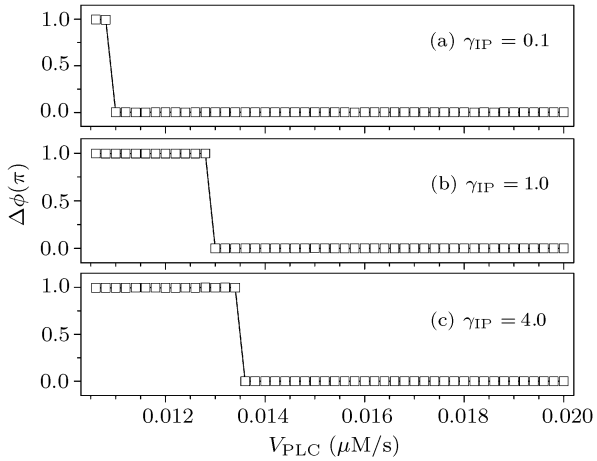


Fig. 2. Dependence of $\Delta\phi$ on $V_{\rm PLC}$ for three different coupling intensities $\gamma_{\rm IP}$ in the absence of $\gamma_{\rm Ca}$ for the two coupled hepatocytes.

In Fig. 4, the dependences of $\Delta\phi$ on coupling intensity $\gamma_{\rm IP}$ for three different $V_{\rm PLC}$ are depicted. Obviously, with the increasing of $\gamma_{\rm IP}$ the synchronized oscillatory mode varies from in-phase to anti-phase. Moreover, when $V_{\rm PLC}$ is increased, the region of anti-phase synchronization shrinks, and then vanishes when $V_{\rm PLC} \geq 0.135\,\mu$M/s. (not shown in Fig. 4)

Finally, we investigate the influence of coupling strength $\gamma_{\rm Ca}$ on synchronization of intracellular Ca^{2+} oscillations. The phase diagrams in two-dimensional parameter space of $\gamma_{\rm IP}$ and $V_{\rm PLC}$ for four different $\gamma_{\rm Ca}$ are plotted in Fig. 5. The horizontal axis denotes the synthesis velocity of IP_3 varying from $0.0106\,\mu$M/s to $0.02\,\mu$ M/s, and the vertical axis corresponds to $\gamma_{\rm IP}$ varying from 0.1 to 5.0. The shaded region describes anti-phase synchronization, and the whitened region describes the in-phase one. One can see that when $\gamma_{\rm Ca}$ is increased, the anti-phase region shrinks quickly; this reveals that the coupling strength $\gamma_{\rm Ca}$ restrains the anti-phase synchronous behaviour but facilitates the in-phase one. Furthermore, when $\gamma_{\rm Ca}$ is raised to some extent, the anti-phase synchronization disappears.

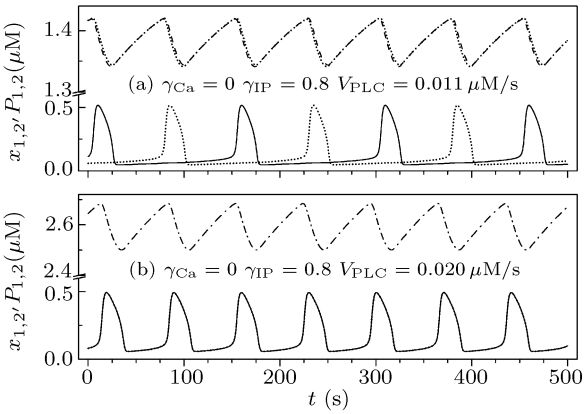


Fig. 3. Typical oscillations of Ca^{2+} and IP_3 in a pair of coupled cells. Solid line and dot-dashed line denote x_1 and x_2, respectively. Dashed line represents $P_{1,2}$, $\gamma_{\rm Ca} = 0$. (a) Anti-phase synchronization, (b) in-phase synchronization.

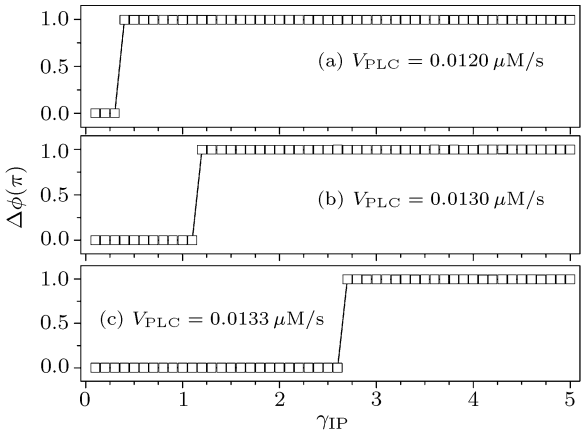


Fig. 4. Dependence of $\Delta\phi$ on coupling intensity $\gamma_{\rm IP}$ for three different $V_{\rm PLC}$ in the absence of $\gamma_{\rm Ca}$ for the two coupled hepatocytes.

In fact, we may find some useful clues to explain the anti-phase and in-phase synchronous behaviour from the model itself. Recent theoretical and experimental studies also gave similar results.[20,21] On the one hand, the first formula of Eqs. (1) and (2) tells us that the influx $J_{\rm in}$ includes the constant leak v_0 and Ca^{2+} entry which depends on IP_3 concentration. Here IP_3 described in the third formula of Eqs. (1) includes the effects of $V_{\rm PLC}$ and IP_3, so the average concentration of IP_3 is changed by the varying of $V_{\rm PLC}$. Thus, for a single cell case, the model has one steady state for small and large value of $V_{\rm PLC}$, while for a proper range of $V_{\rm PLC}(0.0106 \sim 0.045\,\mu$M/s) there exist two Hopf bifurcation points, and the amplitude of calcium

spikes changes slightly whereas the period of cytosolic calcium oscillations (right axis) decreases with increasing of $V_{\rm PLC}$ (see Fig. 1). On the other hand, we can also find from Fig. 3 that the Ca^{2+} oscillations are accompanied by oscillations in IP_3 with different phases. According to Fig. 1, some researchers found that near the supercritical HB(LBP), there exist some concomitant oscillation branches, and the Ca^{2+} in the couplets can oscillate with the same period, and jump back and forth between anti-phase and in-phase synchronized states.[21] Of course, such jumping behaviour depends on the coupling strength of IP_3 and Ca^{2+}. In the absence of $\gamma_{\rm Ca}$(see Figs. 2 and 4), the phase difference approaches π for small $V_{\rm PLC}$, in this case, the two cells exhibit anti-phase synchronized states (APSS). However, for larger $V_{\rm PLC}$ the phase difference decrease to 0 sharply, hence the two cells locked in-phase Ca^{2+} oscillations. One can observe the region of APSS is enlarged for bigger $\gamma_{\rm IP}$. However, if the gap junctional coupling of Ca^{2+} diffusion is considered (see Fig. 5), although it is smaller than IP_3 diffusion, APSS region shrinks quickly due to the fast Ca^{2+} diffusion effect.

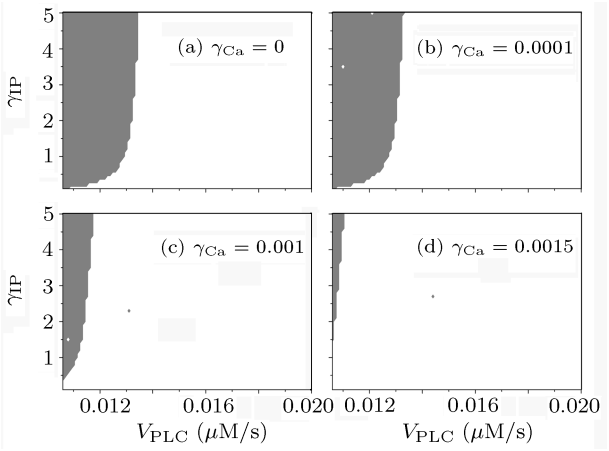


Fig. 5. Phase diagrams in $V_{\rm PLC}$-$\gamma_{\rm IP}$ plane for different $\gamma_{\rm Ca}$ in the two coupled hepatocytes.

In conclusion, we have theoretically investigated the synchronized behaviour of Ca^{2+} oscillations in a pair of hepatocytes. It is shown that comparatively low extracellular stimulation that is close to Hopf bifurcation is necessary for the occurrence of anti-phase synchronization. Gap junction to IP_3, on the other hand, is effective in anti-phase oscillations, while gap junction to Ca^{2+} destroys this synchronization. Our conclusions are highlighted in the context of anti-phase Ca^{2+} oscillations. To our knowledge, there have been few reports on anti-phase synchronization of calcium oscillations in theoretical work.[20] However, recent experimental results have exhibited that anti-phase synchronization of calcium oscillations does indeed exist.[22] Anti-phase Ca^{2+} oscillations may reveal an alternative approach of intercellular calcium signal transmissions in biological systems. In this study, our simulation only gives a possible way of controlling synchronous effects in the coupled system. We hope that our findings can not only contribute to the understanding of the synchronous mechanism of intercellular calcium signalling, but also arouse new interest of scientists in associated fields. Further experimental and theoretical work will be helpful to future research.

References

[1] Alberts B, Bray D, Lewis J, Raff M, Roberts K and Watson J D 1994 *Molecular Biology of the Cell* (New York: Garland)
[2] Kandel E R, Schwartz J H and Jessel T M 1991 *Principles of neural science* (Norwalk, CT: Appleton and Lange)
[3] Shi X M and Liu Z R 2005 *Chin. Phys. Lett.* **22** 3206
[4] Höfer T 1999 *Biophys. J.* **77** 1244
[5] Dupont G, Tordjmann T, Clair C, Swillens S, Claret M and Combettes L 2000 *FASEB J.* **14** 279
[6] Robb L D and Thomas A P 1995 *J. Biol. Chem.* **270** 8102
[7] Tordjmann T, Berthon B, Claret M and Combettes L 1997 *EMBO J.* **16** 5398
Tordjmann T, Berthon B, Jacquemin E, Clair C, Stelly N, Guillon G, Claret M and Combettes L 1998 *EMBO J.* **17** 4695
[8] Zimmermann B and Walz B 1997 *J. Physiol.* **500** 17
[9] Yule D I, Stuenkel E and Williams J A 1996 *Am. J. Physiol.* **271** C1285
[10] Wu D, Jia Y, Zhan X, Yang L J and Liu Q 2005 *Biophys.Chem.* **113** 145
Wu D and Jia Y 2007 *Biophys. Chem.* **125** 247
[11] Politi A, Gaspers L D, Thomas A P and Höfer T 2006 *Biophys. J.* **90** 3120
[12] Schuster S, Marhl M and Höfer T 2002 *Eur. J. Biochem.* **269** 1333
[13] Falcke M 2004 *Adv. Phys.* **53** 255
[14] Ying Y J and Huang Z Q 2001 *Chin. Phys. Lett.* **18** 695
[15] Ying Y J and Li W H 2003 *Chin. Phys. Lett.* **20** 1168
[16] Jia Y, Yang L J, Wu D, Liu Q and Zhan X 2004 *Chin. Phys. Lett.* **21** 1666
[17] Hirose K S, Kadowaki M, Tanabe H, Takeshima and Lino M 1999 *Science* **284** 1527
[18] Young K W, Nash M S, Challiss R A and Nahorski S R 2003 *J. Biol.Chem.* **278** 20753
[19] Dupont G and Erneux C 1997 *Cell Calcium* **22** 321
[20] Bindschadler M and Sneyd J 2001 *Chaos* **11** 237
[21] Ullah G, Jung P and Cornell-B A H 2006 *Cell Calcium* **39** 197
[22] Rahman A, Hughes A, Matchkov V, Nilsson H and Aalkjær C 2007 *Cell Calcium* **42** 536